

Abstract

We present ground-based FTIR (Fourier transform infrared) water vapour analyses performed for three different spectral regions: in the mid-infrared at 790–1330 cm^{-1} and 2650–3180 cm^{-1} as well as in the near infrared at 4560–4710 cm^{-1} . All three analyses allow the retrieval of lower, middle, and upper tropospheric water vapour amounts with a vertical resolution of about 2, 4, and 6 km, respectively. The mid-infrared analyses allow in addition the retrieval of lower and middle/upper tropospheric δD values with a vertical resolution of 3 and 7 km, respectively. The H_2O profiles retrieved in all three spectral regions show a very good agreement with coincident Vaisala RS92 radiosonde measurements performed on seven different days during the Measurements of Humidity in the Atmosphere and Validation Experiment (MOHAVE) 2009 campaign. We analyse 325 ground-based FTIR spectra measured on 11 different days. For optimised line parameters we find that the 325 H_2O profiles retrieved in each of the three spectral regions and the 325 δD profiles retrieved in the two mid-infrared regions agree very well. Spectroscopic parameters are the major error source for the ground-based remote sensing of δD profiles. Our inter-comparison of the two different mid-infrared spectral regions allows thus an empirical estimation of the precision of the remotely-sensed δD data of 10 and 20%, for the lower and middle/upper troposphere, respectively.

1 Introduction

The Fourth Assessment Report of the Intergovernmental Panel on Climate Change describes the insufficient understanding of the atmospheric water cycle as a major source of uncertainties of climate projections (Randall et al., 2007). Atmospheric water cycle research is thus of highest scientific priority for predicting climate change. Climate change research requires continuous, high quality, and consistent long-term observations with good global coverage. In the framework of NDACC (Network for the

AMTD

3, 3105–3132, 2010

H_2O and δD profiles from different spectral regions

M. Schneider et al.

Title Page

Abstract

Introduction

Conclusions

References

Tables

Figures

◀

▶

◀

▶

Back

Close

Full Screen / Esc

Printer-friendly Version

Interactive Discussion



H₂O and δ D profiles from different spectral regions

M. Schneider et al.

Title Page

Abstract

Introduction

Conclusions

References

Tables

Figures



Back

Close

Full Screen / Esc

Printer-friendly Version

Interactive Discussion



spectroscopic parameters are the main error source our paper provides a good empirical error assessment of the FTIR δ D data. This is important since in order to achieve an optimal signal to noise ratio most ground-based FTIR instruments use optical filters and measure the different mid- and near-infrared spectral regions by a sequence of measurements. In this paper we demonstrate that tropospheric H₂O and δ D profiles can be consistently retrieved in different spectral regions. The possibility of applying different spectral regions significantly increases the number of recorded spectra that can be used for ground-based water vapour profile analyses, leading to a denser dataset with good temporal and spatial coverage. A dense dataset is important to study the high variability and the long-term behavior of the tropospheric water vapor distribution. Furthermore, it will assure more coincidences with satellite overpasses, thereby facilitating the still unsatisfactory validation of the space-based near- and mid-infrared sensors with the potential for global tropospheric H₂O and δ D observations: ACE (Atmospheric Chemistry Experiment, Nassar et al., 2007), TES (Tropospheric Emission Spectrometer, Worden et al., 2006a), SCIAMACHY (Scanning Imaging Absorption Spectrometer for Atmospheric Cartography, Frankenberg et al., 2009), and IASI (Infrared Atmospheric Sounding Interferometer, Herbin et al., 2009). These sensors have different sensitivities: ACE, TES, and IASI measure mainly upper and middle tropospheric δ D whereas SCIAMACHY detects column integrated δ D. A comprehensive satellite sensor validation requires δ D profile data, and the ground-based FTIR technique is unique in providing such data on a continuous basis.

In Sect. 2 we give a brief description of the MOHAVE-2009 campaign and the MkIV spectrometer. Section 3 presents the analysed spectral regions and Sect. 4 documents the theoretical performances of the retrievals. Sections 5 and 6 compare the retrievals to coincident radiosonde measurements and between each other. Our study is summarised in Sect. 7.

2 FTIR measurements during MOHAVE-2009

The MOHAVE-2009 campaign took place at the JPL Table Mountain Facility (TMF) in October 2009. For the campaign a large variety of different experiments performed side-by-side water vapour measurements from the ground to the mesopause:

- 3 water vapour Raman lidars: nighttime measurements, vertical range: ground-20 km.
- 15 cryogenic frostpoint hygrometers and 3 frost-point hygrometer radiosondes: during night (in coincidence with lidar observations), vertical range: ground-30 km.
- 50 Vaisala RS92 radiosondes: Mostly during night, vertical range: ground-15 km.
- 2 microwave radiometer: night and day, vertical range: 20–80 km.
- 2 GPS receivers: night and day, only total column amounts.
- FTUVS: daytime measurements, only total column amounts.
- The MkIV FTIR: daytime measurements, vertical range: from the ground to the upper tropopause.

The main focus of the campaign was a further development and a quality assessment of the water vapour lidar technique. Therefore most measurements were performed during night. In addition measurements were performed in coordination with satellite overpasses (Aura MLS, Aura TES, Aqua AIRS, ACE, and MIPAS).

The MkIV FTIR spectrometer was designed and built at the Jet Propulsion Laboratory in 1984. Since then it has been operated on different platforms (ground-, balloon-based, and aircraft-based) in the framework of a large variety of different campaigns mainly dedicated to the investigation of stratospheric ozone chemistry. The MkIV can measure high resolution spectra (maximal optical path difference of 200 cm) and covers

AMTD

3, 3105–3132, 2010

H₂O and δ D profiles from different spectral regions

M. Schneider et al.

Title Page

Abstract

Introduction

Conclusions

References

Tables

Figures

◀

▶

◀

▶

Back

Close

Full Screen / Esc

Printer-friendly Version

Interactive Discussion



a very broad spectral range (650–5650 cm⁻¹), whereby two liquid nitrogen-cooled detectors are applied: an HgCdTe photoconductor (for wavenumbers below 1850 cm⁻¹) and an InSb photodiode for higher wavenumbers. The two detector design prevents photon noise from the high frequencies, where the sun is brighter, from degrading the signals at the lower frequencies. Simultaneous high-resolution measurement over such a wide spectral region imposes severe constraints on the dynamic range and linearity required of the detectors, pre-amplifiers, and signal chains. In the MkIV, this problem is addressed by using of a 18-bit ADC module. More details about the MkIV spectrometer can be found in Toon (1991) and on the web page: <http://mark4sun.jpl.nasa.gov/>.

3 The analysis in different spectral regions

We analyse the spectra with the algorithm PROFFIT (Hase et al., 2004). We perform the retrievals in three different spectral regions where ground-based solar absorption spectra have relatively isolated H₂¹⁶O, H₂¹⁸O, and HD¹⁶O lines of different strength: the 790–1330 cm⁻¹, the 2650–3050 cm⁻¹, and the 4560–4710 cm⁻¹ regions. The fitted spectral microwindows containing the water vapour lines are shown in Figs. 1–3. The Figures show a typical MkIV MOHAVE-2009 measurement with a spectral resolution of about 0.008 cm⁻¹ (OPD_{max}=116.5 cm). In addition, we fit for all retrievals two CO₂ lines of different strength, which allows us to estimate the temperature from the measured spectra (Schneider and Hase, 2008). Due to the large vertical gradient and the large dynamic range of tropospheric water vapour amounts, ground-based water vapour retrievals are very demanding. In order to produce data of good quality we apply the sophisticated recipes presented in Schneider and Hase (2009b). These are: (a) a fit to a variety of water vapour lines with different strength, (b) a logarithmic scale inversion, (c) a speed-dependent Voigt line-shape model, (d) a simultaneous temperature profile retrieval, and (e) the consideration of atmospheric emission for the 790–1330 cm⁻¹ retrieval. For the retrievals in the 790–1330 cm⁻¹ and 2650–3050 cm⁻¹ regions we introduce an H₂¹⁶O-HD¹⁶O (and H₂¹⁶O-H₂¹⁸O) inter-species constraint. This allows an optimal estimation of δD profiles (Schneider et al., 2006b).

H₂O and δD profiles from different spectral regions

M. Schneider et al.

Title Page

Abstract

Introduction

Conclusions

References

Tables

Figures



Back

Close

Full Screen / Esc

Printer-friendly Version

Interactive Discussion



As spectral parameters we use the HITRAN 2008 parameters (Rothman et al., 2009, with 2009 updates), which we slightly modified in order to minimize the systematic differences between the ground-based FTIR profiles and radiosonde data: a modification of 1–2% of the pressure broadening coefficients γ_{air} and of line intensity coefficients I of less than 5%. These modifications are all within the uncertainty ranges given in the HITRAN parameter file and are thus justified. Furthermore, we adapted the line parameters for a speed-dependent Voigt line-shape model, which is recommended for ground-based FTIR water vapour profile remote sensing (Schneider and Hase, 2009a; Schneider et al., 2010c). For further details about the modified HITRAN line parameters applied in this study please refer to (Schneider et al., 2010c).

4 Theoretical performance

Figure 4 shows the averaging kernels for H₂O for the three retrievals and for the typical measurement as shown in Figs. 1–3. In general all three spectral regions offer a similar vertical resolution and sensitivity (sum along the row of the averaging kernel matrix) with respect to tropospheric H₂O. Structures with a width of 2–3, 4, and 6 km can be detected for the lower, middle, and upper troposphere, respectively. There are small differences concerning the sensitivity and vertical resolution: for the 790–1330 cm⁻¹ region the sensitivity is better than 75% from the surface up to an altitude of 11 km, whereas for the 2650–3180 cm⁻¹ and 4560–4710 cm⁻¹ this sensitivity range extends to above 12 km. In the lower troposphere the mid-infrared retrievals provide more detailed profile information when compared to the near infrared retrieval.

Figure 5 depicts the averaging kernels of δD for the mid-infrared retrievals (790–1330 cm⁻¹ and 2650–3180 cm⁻¹). Again, both spectral regions offer a similar vertical resolution but there are slight differences concerning the sensitivity. The natural δD variability is rather small (about 8%). Such a small variability causes only weak spectral signatures and as a consequence the profiles of δD are more difficult to measure than profiles of H₂O. The vertical resolution is limited to about 3 km for the lower troposphere

H₂O and δD profiles from different spectral regions

M. Schneider et al.

Title Page

Abstract

Introduction

Conclusions

References

Tables

Figures



Back

Close

Full Screen / Esc

Printer-friendly Version

Interactive Discussion



and 7 km for the middle/upper troposphere and the sensitivity is larger only than 75% for altitude below about 8.5 and 9 km for the 790–1330 cm⁻¹ and 2650–3180 cm⁻¹ retrievals, respectively.

The trace of the averaging kernel matrix quantifies the amount of information introduced by the measurement. It can be interpreted in terms of degrees of freedom of the measurement (dof). The larger this value the more independent the solution is from the a priori assumptions. Table 1 collects the typical dof values for the retrievals in the different spectral regions. The dof values are between 2 and 3 for H₂¹⁶O and HD¹⁶O. In the middle infrared regions we retrieve both isotopologues, which explains that the typical overall water vapour dof value is about 5 compared to 2.6 in case of the near infrared, where we only retrieve the main isotopologue. In addition in the 2650–3180 cm⁻¹ region we get some information from the H₂¹⁸O isotopologue.

5 H₂O profiles

During MOHAVE-2009 many radiosondes were launched. Although most launches were during night (in order to coincide with the lidar measurements) there were seven Vaisala RS92 measurements performed at the same time as MkIV measurements. The sondes were launched about 350 m from the location of the spectrometer. Therefore, the coincident RS92 in-situ and the MkIV remote sensing experiments detect very similar airmasses, at least at low altitudes.

Figure 6 compares the 7 coincident RS92 and MkIV H₂O profiles (for the 790–1330 cm⁻¹ retrieval): the small black squares show the RS92 profiles after the so-called time-lag, radiation, and empirical corrections were applied (Miloshevich et al., 2004, 2009). These in-situ profiles offer a very high vertical resolution. To the contrary, the remote sensing technique only allows resolving rather rough vertical structures (see averaging kernels of Fig. 4). For an adequate comparison we have to degrade the RS92 profiles to the vertical resolution of the MkIV profiles. Therefore, we convolve the

H₂O and δD profiles from different spectral regions

M. Schneider et al.

Title Page

Abstract

Introduction

Conclusions

References

Tables

Figures

◀

▶

◀

▶

Back

Close

Full Screen / Esc

Printer-friendly Version

Interactive Discussion



spectral regions. The top panels show the correlations between the 790–1330 cm⁻¹ and 2650–3180 cm⁻¹ retrievals and the lower panel between the 4560–4710 cm⁻¹ and 2650–3180 cm⁻¹ retrievals. The correlations are very strong (coefficients ρ are close to 1 throughout the troposphere). Figure 8 proves that the water vapour profiles obtained in the three different spectral regions are very consistent. In all three spectral regions the FTIR system observes almost identical lower, middle, and upper tropospheric water vapour variations.

In Fig. 9 we depict a statistics of the difference between the different water vapour retrievals. The left panel shows the mean and 1 σ standard deviation (black line and error bars) of difference between the 790–1330 cm⁻¹ and 2650–3180 cm⁻¹ retrievals. The mean difference is smaller than 9% throughout the troposphere and the scatter is smaller than 16%. When comparing two remotely-sensed profiles we have to account for differences in the averaging kernels. The H₂O averaging kernels of the 790–1330 cm⁻¹ and 2650–3180 cm⁻¹ retrievals are similar but not identical (see Fig. 4). With a statistics of the difference between the real state x and the climatological mean state x_a represented by the ensemble $\{x - x_a\}$ we can estimate how the differences in the averaging kernels affects our comparison:

$$\{\epsilon_1 - \epsilon_2\} = (\hat{A}_1 - \hat{A}_2)\{x - x_a\} \quad (2)$$

Here \hat{A}_1 and \hat{A}_2 are typical averaging kernels for the 790–1330 cm⁻¹ and the 2650–3180 cm⁻¹ retrieval, respectively. The ensemble $\{\epsilon_1 - \epsilon_2\}$ represents the expected differences between the two retrievals caused by the different averaging kernels (see also Rodgers and Connor, 2003). The grey areas in the graphs of Fig. 9 represent the 1 σ area of the ensemble $\{\epsilon_1 - \epsilon_2\}$. We observe that most of the difference (mean and scatter) between the retrieved H₂O profiles can be explained by the averaging kernels. The profiles are very consistent and if accounting for the different averaging kernels the agreement between the different retrievals is very likely better than 5%. Only the somewhat increased difference between the lower tropospheric amounts obtained from the 4560–4710 cm⁻¹ and 2650–3180 cm⁻¹ retrievals cannot be explained by the averaging

H₂O and δ D profiles from different spectral regions

M. Schneider et al.

Title Page

Abstract

Introduction

Conclusions

References

Tables

Figures

◀

▶

◀

▶

Back

Close

Full Screen / Esc

Printer-friendly Version

Interactive Discussion



kernels. It is very likely due to inconsistencies between the spectroscopic line parameters of these two spectral regions.

6 δD profiles

Besides the ground-based FTIR there is no other MOHAVE-2009 experiment with the capability to measure tropospheric δD profiles. So we cannot perform a comparison as shown in Figs. 6 and 7 for the H_2O profiles. Instead we compare statistics. The grey area in Fig. 10 represents the 1σ range of subtropical δD in-situ measurements performed by Ehhalt (1974) and Zahn (2001). Superimposed are statistics of δD as retrieved from the MOHAVE-2009 MkIV spectra. The red line shows the mean and the 1σ standard deviation for all the 325 δD profiles retrieved in the $790\text{--}1330\text{ cm}^{-1}$ region, the blue line and error bars show the same but for the $2650\text{--}3180\text{ cm}^{-1}$ retrievals. In both spectral regions we observe the monotonic decrease of δD values between the lower and upper troposphere. Since small inconsistencies between the $HD^{16}O$ and $H_2^{16}O$ line parameters would significantly change the retrieved δD profile shape (Schneider et al., 2006b), Fig. 10 suggests that the modified HITRAN 2008 $HD^{16}O$ and $H_2^{16}O$ line parameters given by Schneider et al. (2010c) are quite consistent.

In Fig. 11 we depict correlations between the δD values obtained by the retrievals in the two mid-infrared spectral regions. The agreement is very satisfactory. Please keep in mind that the axis are in the ‰ scale, i.e. Fig. 11 shows variations of a few percent only. Such small variation are very challenging for a remote sensing system. Nevertheless, we observe that for both spectral regions the same small variation in δD are detected. Keeping in mind that uncertainties in the spectroscopic parameters are the major error source for ground-based δD remote sensing (Schneider et al., 2006b), the strong correlation between the δD profiles retrieved in two different spectral regions is a robust demonstration of the quality of these profiles.

H_2O and δD profiles from different spectral regions

M. Schneider et al.

Title Page

Abstract

Introduction

Conclusions

References

Tables

Figures



Back

Close

Full Screen / Esc

Printer-friendly Version

Interactive Discussion



Figure 12 shows the mean and standard deviation for the 325 δD profiles retrieved in the two mid-infrared regions. The mean difference is very low in the lower troposphere (mean and 1σ standard deviation of smaller than 10‰). It is largest in the middle/upper troposphere (at 9 km it is about 25‰). A part of these differences is caused by the slightly different averaging kernels (the grey area shows the estimation according to Eq. 2). The difference is the sum of the errors from both retrievals. Assuming a certain independence of the retrievals we can conclude that each retrieval produces lower and middle/upper tropospheric δD with a precision of better than 10 and 20‰, respectively.

7 Conclusions

We show that tropospheric H_2O and δD profiles can be obtained from infrared solar absorption spectra recorded in different spectral regions. The mid-infrared regions ($790\text{--}1330\text{ cm}^{-1}$ and the $2650\text{--}3180\text{ cm}^{-1}$) are measured regularly by the NDACC ground-based FTIR spectrometers, whereas the near infrared region ($4560\text{--}4710\text{ cm}^{-1}$) is covered by the TCCON spectrometers. Concerning H_2O all three spectral regions allow the distinction between lower, middle, and upper tropospheric water vapour according to the averaging kernels of Fig. 4. During the MOHAVE-2009 campaign the agreement with the Vaisala RS92 radiosonde profiles is within 20%. When applying optimised spectroscopic parameters the different water vapour profiles are very consistent. The agreement between the retrievals is very likely better than 5% throughout the troposphere. Therefore, we can collect the water vapour profiles obtained in the different spectral regions in a single database. Such a collection of long-term continuous water vapour profile data is important for satellite validation and long-term climate studies.

In both mid-infrared regions we can detect δD profiles and distinguish between the lower and middle/upper tropospheric δD variability. There are no reference δD profile measurements made in coincidence with the FTIR measurements and an empirical validation of the FTIR δD profiles is difficult. At least the FTIR data are in good agreement with climatological data obtained from a variety of in-situ measurements. Furthermore,

H_2O and δD profiles from different spectral regions

M. Schneider et al.

Title Page

Abstract

Introduction

Conclusions

References

Tables

Figures

◀

▶

◀

▶

Back

Close

Full Screen / Esc

Printer-friendly Version

Interactive Discussion



H₂O and δ D profiles from different spectral regions

M. Schneider et al.

Title Page

Abstract

Introduction

Conclusions

References

Tables

Figures

◀

▶

◀

▶

Back

Close

Full Screen / Esc

Printer-friendly Version

Interactive Discussion



the δ D profiles from both spectral regions are very consistent: we observe a 1σ scatter between both retrievals of 10 and 25‰ in the lower and middle/upper troposphere, respectively. Most of this scatter can be explained by differences in the vertical resolution of the δ D profiles from the two spectral regions. Theoretically, the leading error source of ground-based FTIR δ D profiles are deficits in the spectroscopic line parameters. Therefore, the good agreement between retrievals performed in two different spectral regions can be interpreted as a first empirical error assessment. Our study suggests that 10 and 20‰ is an upper estimate of the FTIR's lower and middle/upper tropospheric δ D precision. This is very satisfactory and underlines the large potential of the NDACC FTIR measurements in the field of water cycle research and confirms their essential role for validating the different space-based tropospheric δ D measurements.

Acknowledgements. M. Schneider has been supported by the Deutsche Forschungsgemeinschaft via the project RISOTO (Geschäftszeichen SCHN 1126/1-1 and 1-2). We are grateful to the Goddard Space Flight Center for providing the temperature and pressure profiles of the National Centers for Environmental Prediction via the automailer system. Part of this work was performed at the Jet Propulsion Laboratory, California Institute of Technology under contract with NASA.

References

- Ehhalt, D. H.: Vertical profiles of HTO, HDO, and H₂O in the Troposphere, Rep. NCAR-TN/STR-100, Natl. Cent. for Atmos. Res., Boulder, Colo., 1974. 3115, 3130
- Frankenberg, C., Yoshimura, K., Warneke, T., Aben, I., Butz, A., Deutscher, N., Griffith, D., Hase, F., Notholt, J., Schneider, M., Schreyver, H., and Röckmann, T.: Dynamic processes governing lower-tropospheric HDO/H₂O ratios as observed from space and ground, *Science*, 325, 1374–1377, doi:10.1126/science.1173791, 2009. 3108
- Hase, F., Hannigan, J. W., Coffey, M. T., Goldman, A., Höpfner, M., Jones, N. B., Rinsland, C. P., and Wood, S. W.: Intercomparison of retrieval codes used for the analysis of high-resolution, ground-based FTIR measurements, *J. Quant. Spectrosc. Ra.*, 87, 25–52, 2004. 3110
- Herbin, H., Hurtmans, D., Clerbaux, C., Clarisse, L., and Coheur, P.-F.: H₂¹⁶O and HDO mea-

H₂O and δD profiles from different spectral regions

M. Schneider et al.

Title Page

Abstract

Introduction

Conclusions

References

Tables

Figures

◀

▶

◀

▶

Back

Close

Full Screen / Esc

Printer-friendly Version

Interactive Discussion



surements with IASI/MetOp, Atmos. Chem. Phys., 9, 9433–9447, doi:10.5194/acp-9-9433-2009, 2009. 3108

Kurylo, M. J. and Zander, R.: The NDSC – Its status after 10 years of operation, Proceedings of XIX Quadrennial Ozone Symposium, Hokkaido University, Sapporo, Japan, 167–168, 2000. 3107

Miloshevich, L. M., Paukkunen, H., Vömel, H., and Oltmans, S. J.: Development and validation of a time lag correction for Vaisala radiosonde humidity measurements, J. Atmos. Ocean. Technol., 21, 1305–1327, 2004. 3112

Miloshevich, L. M., Vömel, H., Whiteman, D. W., and Leblanc, T.: Accuracy assessment and correction of Vaisala RS92 radiosonde water vapor measurements, J. Geophys. Res., 114, D11305, doi:10.1029/2008JD011565, 2009. 3112, 3126

Nassar, R., Bernath, P. F., Boone, C. D., Gettelman, A., McLeod, S. D., and Rinsland, C. P.: Variability in HDO/H₂O abundance ratios in the tropical tropopause layer, J. Geophys. Res., 112, D21305, doi:10.1029/2007JD008417, 2007. 3108

Randall, D. A., Wood, R. A., Bony, S., Colman, R., Fichet, T., Fyfe, J., Kattsov, V., Pitman, A., Shukla, J., Srinivasan, J., Stouffer, R. J., Sumi, A., and Taylor, K. E.: Climate Models and Their Evaluation, In: Climate Change 2007: The Physical Science Basis, Contribution of Working Group I to the Fourth Assessment Report of the Intergovernmental Panel on Climate Change, edited by: Solomon, S., Qin, D., Manning, M., Chen, Z., Marquis, M., Averyt, K. B., Tignor, M., and Miller, H. L., Cambridge University Press, Cambridge, UK and New York, 2007. 3106

Rodgers, C. D. and Connor, B. J.: Intercomparison of remote sounding instruments, J. Geophys. Res., 108, 4116, doi:10.1029/2002JD002299, 2003. 3114

Rothman, L. S., Gordon, I. E., Barbe, A., Chris Benner, D., Bernath, P. F., Birk, M., Boudon, V., Brown, L. R., Campargue, A., Champion, J.-P., Chance, K., Coudert, L. H., Dana, V., Devi, V. M., Fally, S., Flaud, J.-M., Gamache, R. R., Goldman, A., Jacquemart, D., Kleiner, I., Lacombe, N., Lafferty, W. J., Mandin, J.-Y., Massie, S. T., Mikhailenko, S. N., Miller, C. E., Moazzen-Ahmadi, N., Naumenko, O. V., Nikitin, A. V., Orphal, J., Perevalov, V. I., Perrin, A., Predoi-Cross, A., Rinsland, C. P., Rotger, M., Simecková, M., Smith, M. A. H., Sung, K., Tashkun, S. A., Tennyson, J., Toth, R. A., Vandaele, A. C., and Vander-Auwera, J.: The HITRAN 2008 molecular spectroscopic database, J. Quant. Spectrosc. Ra., 110, 533–572, doi:10.1016/j.jqsrt.2009.02.013, 2009. 3111

Schneider, M., Hase, F., and Blumenstock, T.: Water vapour profiles by ground-based FTIR

**H₂O and δ D profiles
from different
spectral regions**

M. Schneider et al.

[Title Page](#)[Abstract](#)[Introduction](#)[Conclusions](#)[References](#)[Tables](#)[Figures](#)[◀](#)[▶](#)[◀](#)[▶](#)[Back](#)[Close](#)[Full Screen / Esc](#)[Printer-friendly Version](#)[Interactive Discussion](#)

spectroscopy: study for an optimised retrieval and its validation, *Atmos. Chem. Phys.*, 6, 811–830, doi:10.5194/acp-6-811-2006, 2006. 3107

Schneider, M., Hase, F., and Blumenstock, T.: Ground-based remote sensing of HDO/H₂O ratio profiles: introduction and validation of an innovative retrieval approach, *Atmos. Chem. Phys.*, 6, 4705–4722, doi:10.5194/acp-6-4705-2006, 2006. 3107, 3110, 3115

Schneider, M. and Hase, F.: Technical Note: Recipe for monitoring of total ozone with a precision of around 1 DU applying mid-infrared solar absorption spectra, *Atmos. Chem. Phys.*, 8, 63–71, doi:10.5194/acp-8-63-2008, 2008. 3110

Schneider, M. and Hase, F.: Improving spectroscopic line parameters by means of atmospheric spectra: theory and example for water vapour and solar absorption spectra, *J. Quant. Spectrosc. Ra.*, 110, 1825–1839, doi:10.1016/j.jqsrt.2009.04.011, 2009a. 3107, 3111

Schneider, M. and Hase, F.: Ground-based FTIR water vapour profile analyses, *Atmos. Meas. Tech.*, 2, 609–619, doi:10.5194/amt-2-609-2009, 2009. 3107, 3110

Schneider, M., Romero, P. M., Hase, F., Blumenstock, T., Cuevas, E., and Ramos, R.: Continuous quality assessment of atmospheric water vapour measurement techniques: FTIR, Cimel, MFRSR, GPS, and Vaisala RS92, *Atmos. Meas. Tech.*, 3, 323–338, doi:10.5194/amt-3-323-2010, 2010.

Schneider, M., Yoshimura, K., Hase, F., and Blumenstock, T.: The ground-based FTIR network's potential for investigating the atmospheric water cycle, *Atmos. Chem. Phys.*, 10, 3427–3442, doi:10.5194/acp-10-3427-2010, 2010. 3107

Schneider, M., Hase, F., Blavier, J.-F., Toon, G. C., and Leblanc, T.: An empirical study on the importance of a speed-dependent Voigt line-shape model in different water vapor bands, submitted to *J. Quant. Spectrosc. Ra.*, 2010c. 3111, 3115

Toon, G. C.: The JPL MkIV interferometer, *Opt. Photonics News*, 2, 19–21, 1991. 3110

Worden, J. R., Bowman, K., Noone, D., Beer, R., Clough, S., Eldering, A., Fisher, B., Goldman, A., Gunson, M., Herman, R., Kulawik, S. S., Lampel, M., Luo, M., Osterman, G., Rinsland, C., Rodgers, C., Sander, S., Shephard, M., and Worden, H.: TES observations of the tropospheric HDO/H₂O ratio: retrieval approach and characterization, *J. Geophys. Res.*, 111(D16), D16309, doi:10.1029/2005JD006606, 2006. 3108

Zahn, A.: Constraints on 2-way transport across the Arctic Tropopause based on O₃, stratospheric tracer (SF₆) Ages, and water vapor isotope (D, T) tracers, *J. Atmos. Chem.*, 39, 303–325, 2001. 3115, 3130

**H₂O and δ D profiles
from different
spectral regions**

M. Schneider et al.

Title Page

Abstract

Introduction

Conclusions

References

Tables

Figures

◀

▶

◀

▶

Back

Close

Full Screen / Esc

Printer-friendly Version

Interactive Discussion

**Table 1.** Typical degree of freedoms (dof) with respect to water vapour for the measurements in the different spectral regions.

Spectral range	Dof	Isotopologues
790–1330 cm ⁻¹	4.8	H ₂ ¹⁶ O, HD ¹⁶ O
2650–3180 cm ⁻¹	5.2	H ₂ ¹⁶ O, H ₂ ¹⁸ O, HD ¹⁶ O
4560–4710 cm ⁻¹	2.6	H ₂ ¹⁶ O

H₂O and δ D profiles from different spectral regions

M. Schneider et al.

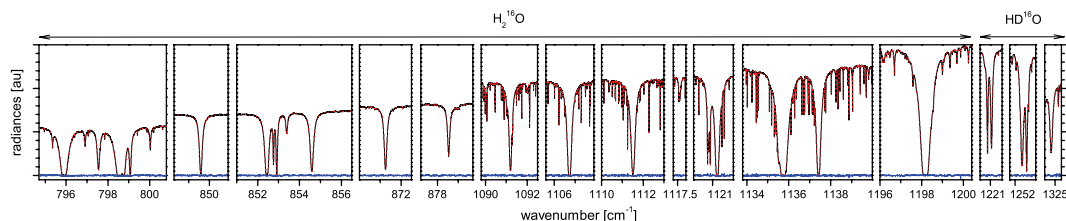


Fig. 1. Spectral microwindows of the 790–1330 cm⁻¹ retrieval taken from a spectra measured on the 18 October 2009, at a solar elevation of 17.8°, and for a total water vapour column amount of 5 mm. Black line: measured spectrum; red line: simulated spectrum; blue line: residuals (difference between measurement and simulation).

[Title Page](#)[Abstract](#)[Introduction](#)[Conclusions](#)[References](#)[Tables](#)[Figures](#)[◀](#)[▶](#)[◀](#)[▶](#)[Back](#)[Close](#)[Full Screen / Esc](#)[Printer-friendly Version](#)[Interactive Discussion](#)

H₂O and δD profiles from different spectral regions

M. Schneider et al.

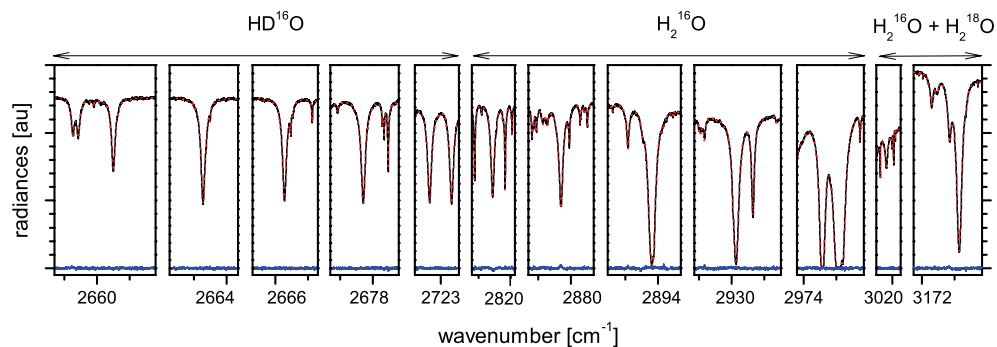


Fig. 2. Same as Fig. 1 but for the 2650–3180 cm⁻¹ region.

[Title Page](#)[Abstract](#)[Introduction](#)[Conclusions](#)[References](#)[Tables](#)[Figures](#)[◀](#)[▶](#)[◀](#)[▶](#)[Back](#)[Close](#)[Full Screen / Esc](#)[Printer-friendly Version](#)[Interactive Discussion](#)

**H₂O and δ D profiles
from different
spectral regions**

M. Schneider et al.

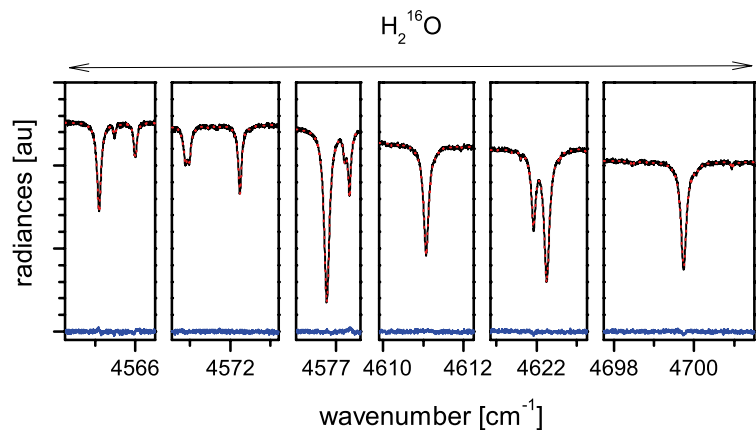


Fig. 3. Same as Fig. 1 but for the 4560–4710 cm^{-1} region.

Title Page

Abstract

Introduction

Conclusions

References

Tables

Figures

◀

▶

◀

▶

Back

Close

Full Screen / Esc

Printer-friendly Version

Interactive Discussion



H₂O and δ D profiles from different spectral regions

M. Schneider et al.

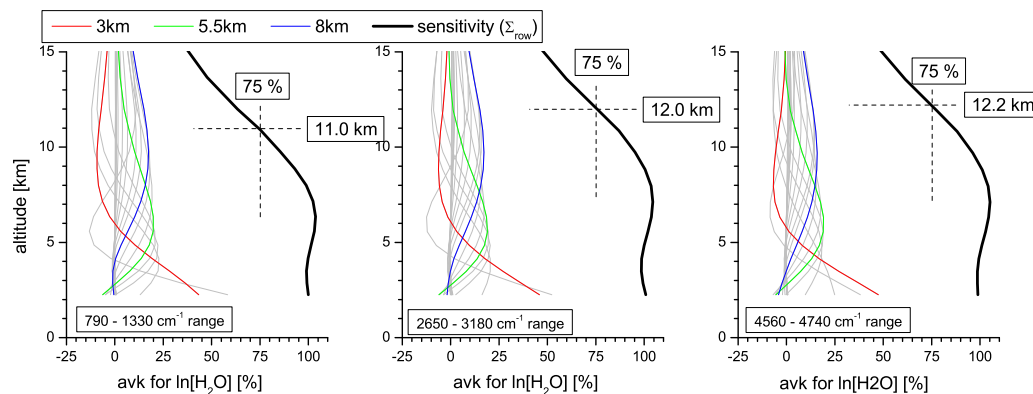


Fig. 4. Averaging kernels for $\ln[\text{H}_2\text{O}]$ for the three analysed spectral regions. Grey lines: kernels for all atmospheric model grid levels; red, green, and blue lines: kernels for the 3, 5.5, and 8 km grid level (representative for the lower, middle, and upper troposphere), respectively; thick black line: sensitivity (sum along the row of the averaging kernel matrix).

Title Page

Abstract

Introduction

Conclusions

References

Tables

Figures

◀

▶

◀

▶

Back

Close

Full Screen / Esc

Printer-friendly Version

Interactive Discussion



H₂O and δ D profiles from different spectral regions

M. Schneider et al.

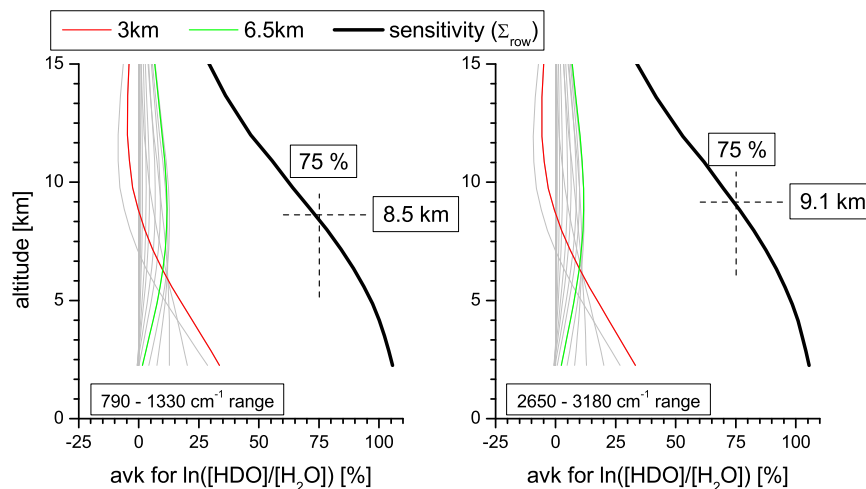


Fig. 5. Averaging kernels for δ D (expressed as $\ln \frac{[\text{HDO}]}{[\text{H}_2\text{O}]}$) for the mid-infrared spectral regions (790–1330 cm⁻¹ and 2650–3180 cm⁻¹). Grey lines: kernels for all atmospheric model grid levels; red and green lines: kernels for the 3 and 6.5 km grid level (representative for the lower and middle/upper troposphere); thick black line: sensitivity (sum along the row of the averaging kernel matrix).

H₂O and δ D profiles from different spectral regions

M. Schneider et al.

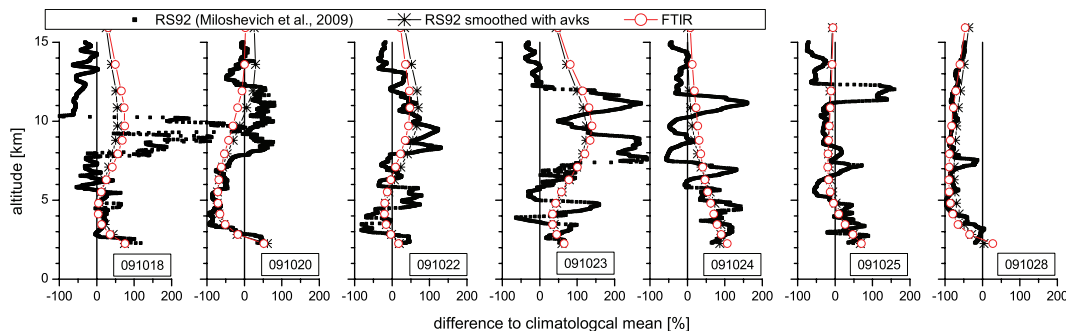


Fig. 6. Comparison of the seven coincident FTIR and Vaisala RS92 H₂O measurements made during MOHAVE-2009 (18, 20, 22, 23, 24, 25, and 28 October 2009). Profiles are presented as percentage difference to a subtropical climatological profile, FTIR profiles are for a retrieval in the 790–1330 cm⁻¹ region. black squares: RS92 data corrected by the Miloshevich et al. (2009) method; black stars: RS92 smoothed with FTIR averaging kernels; Red circles: FTIR.

Title Page

Abstract

Introduction

Conclusions

References

Tables

Figures

◀

▶

◀

▶

Back

Close

Full Screen / Esc

Printer-friendly Version

Interactive Discussion



H₂O and δ D profiles from different spectral regions

M. Schneider et al.

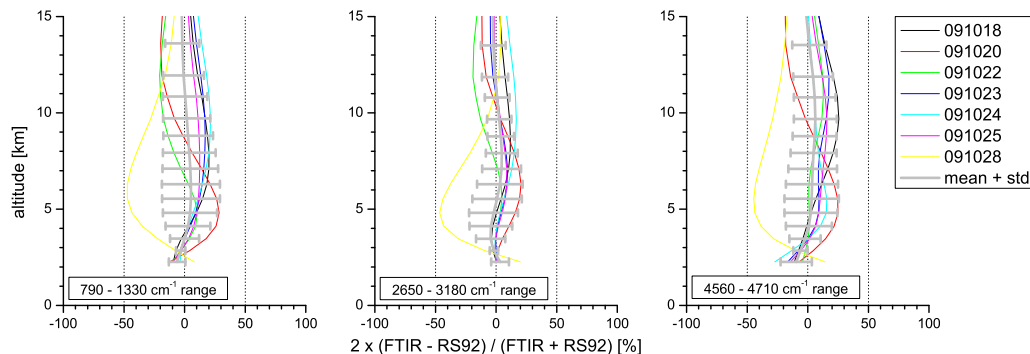


Fig. 7. Difference between coincident FTIR and smoothed RS92 H₂O profiles for the retrievals in the three spectral regions. Coloured lines: individual coincidences; thick grey line and error bars: mean and standard deviation.

[Title Page](#)[Abstract](#)[Introduction](#)[Conclusions](#)[References](#)[Tables](#)[Figures](#)[⏪](#)[⏩](#)[◀](#)[▶](#)[Back](#)[Close](#)[Full Screen / Esc](#)[Printer-friendly Version](#)[Interactive Discussion](#)

H₂O and δD profiles from different spectral regions

M. Schneider et al.

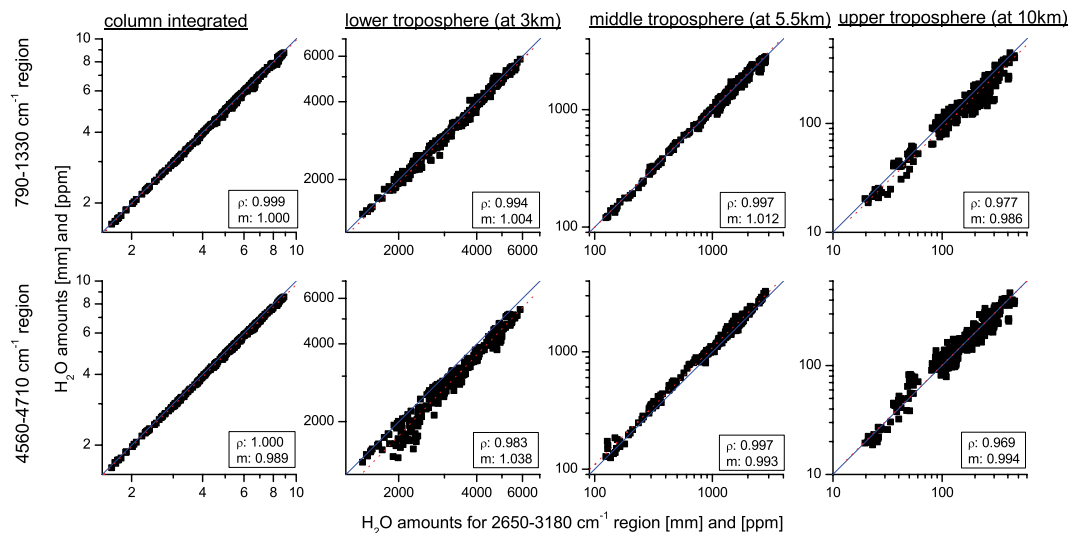


Fig. 8. Correlation between the 325 H₂O profile retrievals for the different spectral regions. Top panels: 790–1330 cm⁻¹ region (y-axes) versus 2650–3180 cm⁻¹ region (x-axis); bottom panels: 4560–4710 cm⁻¹ region (y-axes) versus 2650–3180 cm⁻¹ region (x-axis). From left to right: total column amounts (in mm), volume mixing ratios (in ppm) for the lower, middle, and upper troposphere. The correlation coefficient ρ and the slope of the linear regression line m are written in each panel.

Title Page

Abstract

Introduction

Conclusions

References

Tables

Figures

◀

▶

◀

▶

Back

Close

Full Screen / Esc

Printer-friendly Version

Interactive Discussion



H₂O and δ D profiles from different spectral regions

M. Schneider et al.

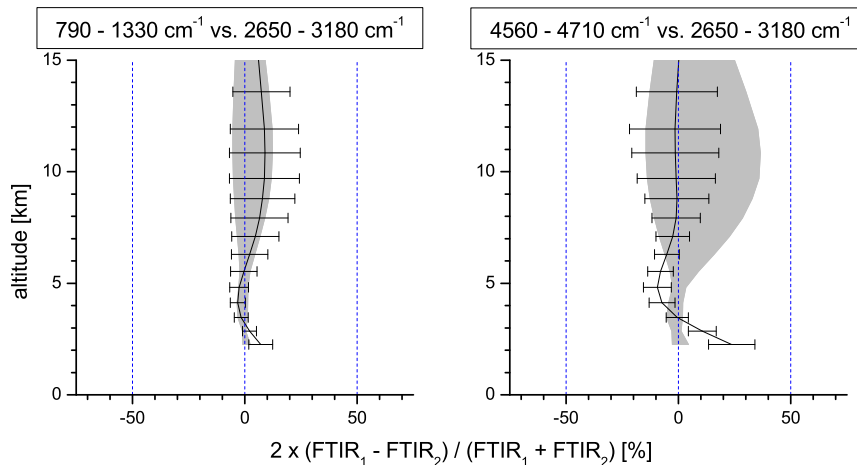


Fig. 9. Difference between the H₂O profiles retrieved in different spectral regions. Left panel: difference between 790–1330 cm⁻¹ and 2650–3180 cm⁻¹ region; right panel: difference between 4560–4710 cm⁻¹ and 2650–3180 cm⁻¹ region. Black line and error bars mean: 1 σ standard deviation of the differences between the 325 retrievals; grey area: theoretical differences due to different averaging kernels (see Eq. 2).

Title Page

Abstract

Introduction

Conclusions

References

Tables

Figures

◀

▶

◀

▶

Back

Close

Full Screen / Esc

Printer-friendly Version

Interactive Discussion



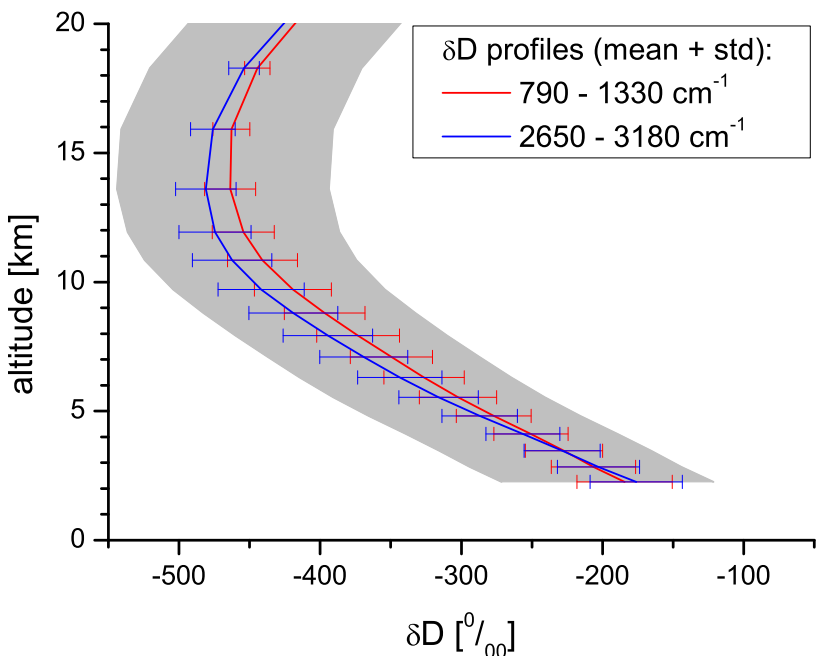


Fig. 10. Statistics of subtropical δD profiles: grey area: 1σ range of δD measured typically in the subtropics (Ehhalt, 1974; Zahn, 2001); lines and error bars: mean and 1σ standard deviation of the 325 MOHAVE-2009 FTIR retrievals; red: in the $790\text{--}1330\text{ cm}^{-1}$ region; blue: in the $2650\text{--}3050\text{ cm}^{-1}$ region.

H₂O and δD profiles from different spectral regions

M. Schneider et al.

Title Page

Abstract Introduction

Conclusions References

Tables Figures

◀ ▶

◀ ▶

Back Close

Full Screen / Esc

Printer-friendly Version

Interactive Discussion



H₂O and δ D profiles from different spectral regions

M. Schneider et al.

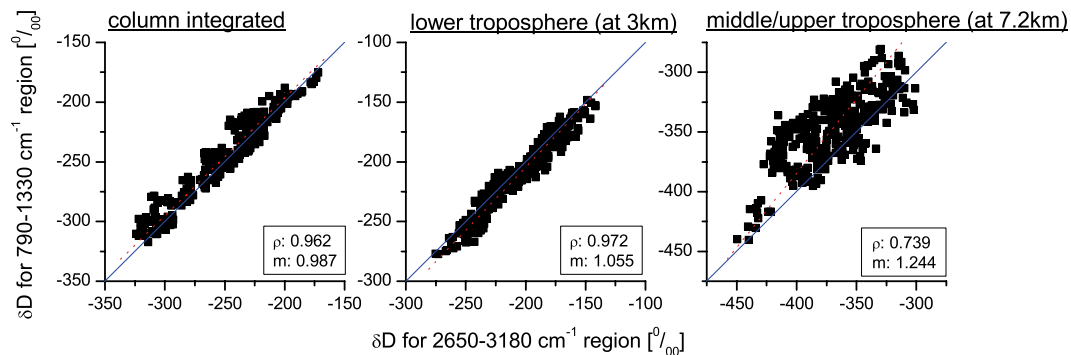


Fig. 11. Same as top panels of Fig. 8 but for δ D profile retrievals and for column integrated, lower, and middle/upper tropospheric δ D (from left to right).

Title Page

Abstract

Introduction

Conclusions

References

Tables

Figures

◀

▶

◀

▶

Back

Close

Full Screen / Esc

Printer-friendly Version

Interactive Discussion



H₂O and δ D profiles from different spectral regions

M. Schneider et al.

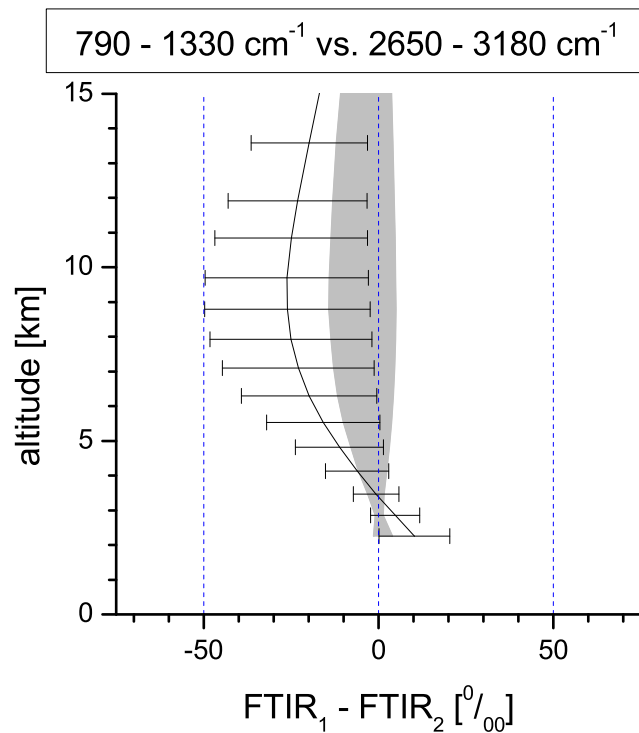


Fig. 12. Same as Fig. 9, but for δ D profiles retrieved in the 790–1330 cm⁻¹ and 2650–3180 cm⁻¹ regions.

Title Page

Abstract

Introduction

Conclusions

References

Tables

Figures

◀

▶

◀

▶

Back

Close

Full Screen / Esc

Printer-friendly Version

Interactive Discussion

